Int. J. Electrochem. Sci., 15**(2020)** 8971 – 8978, doi: 10.20964/2020.09.11

International Journal of ELECTROCHEMICAL SCIENCE
www.electrochemsci.org

Short Communication

Synthesis of Polypyrrole Coated RGO/S Composite as a Cathode material for Enhanced Lithium-Sulfur Batteries

Haishen Song[1,2,3,*], *Hailiang Yuan*[1], *Hezhang Chen*[1], *Guorong Xu*[1], *Anping Tang*[2], *and Lihua Liu*[3]

[1] School of Chemistry and Chemical Engineering, Hunan University of Science and Technology, Xiangtan 411201, Hunan, China
[2] Key Laboratory of Theoretical Organic Chemistry and Functional Molecule of Ministry of Education; Hunan Provincial Key Lab of Advanced Materials for New Energy Storage and Conversion
[3] Hunan Provincial Key Laboratory of Controllable Preparation and Functional Application of Fine Polymers; Hunan Province College Key Laboratory of QSAR/QSPR
[*]E-mail: Song_shs@126.com.

Received: 1 May 2020 / *Accepted:* 15 June 2020 / *Published:* 10 August 2020

Lithium-sulfur (Li-S) batteries have been widely studied in recent years, but the utilization of sulfur cathode is still limited by the low conductivity of cathode material and dissolution of polysulfides. A polypyrrole (PPy) coated reduced graphene oxide/S (RGO/S@PPy) material was synthesized in this study. It is shown that sulfur is uniformly distributed on RGO sheets, and a PPy layer is homogeneously coated on the surface of the RGO/S composite. The PPy coating relieves the dissolution of polysulfides and improves the utilization of active sulfur. As a result, a discharge capacity of 631 mA h g^{-1} after 300 cycles at 0.2C and an excellent rate capability are obtained.

Keywords: Lithium-sulfur battery; Reduced graphene oxide; Polypyrrole; Cycle stability; Rate performance

1. INTRODUCTION

The rapid development of electronic devices and electric vehicles has promoted the increasing need for advanced energy storage equipment with high capacity and high energy/power density[1-5]. Among various candidates, Li-S batteries have attracted much attention because of their high theoretical capacity (1675 mAh g^{-1}), high specific energy density (2600 Wh kg^{-1}), low cost and environmental friendliness [6-9]. Despite these advantages, the low conductivity of polysulfides, the shuttling problem and the volume expansion of cathode material during the charge/discharge process still limit the application of sulfur cathodes [10-13]. Therefore, novel material design strategies must be developed to alleviate the above problems.

Significant studies have been conducted to overcome these problems through encapsulating

sulfur in conductive matrices with plenty of pores and a high specific surface area[14-16]. Among various conductive matrices, porous carbonaceous materials have attracted considerable attention for preparing sulfur-based composites due to their excellent conductivity and various nanostructures [17-20]. Nevertheless, nonpolar carbon materials fail to adequately inhibit the dissolution of polar polysulfides during long-term cycling [21,22]. Conducting polymers have also drawn much attention because of their functional groups and special chemical bonds with sulfur, which are beneficial for high-performance Li-S batteries [23,24]. Polymer/carbon matrix/S composites such as sulfur/graphene/PPy [25], sulfur/carbon nanotubes/PANI [26] and sulfur/acetylene black/PPy [27] have been widely studied in recent years. Meanwhile, uniformly dispersing sulfur nanoparticles into carbon matrices by a wet chemical reaction has been reported to be a more efficient way for addressing shuttling and cycling problems than the well-studied melting-diffusion method[21,28].

Herein, we present a facile synthesis of a ternary RGO/S@PPy composite via deposition of sulfur nanoparticles on RGO and subsequent polymerization of the PPy layer on an RGO/S binary composite. In the material, sulfur is uniformly distributed on RGO sheets, and a PPy layer is coated on the RGO/S composite, resulting in improved cycling stability and rate performance. As a result, a capacity of 631 mA h g^{-1} after 300 cycles and an excellent rate capability are obtained.

2. EXPERIMENTAL

2.1 Synthesis of RGO/S and RGO/S@PPy composites

GO was prepared from natural graphite powder by a modified Hummers method [29]. The RGO/S nanocomposite was synthesized via an insitu solution deposition process. First, 2.43 g of Na_2SO_3 and 3.0 g of $Na_2S{\cdot}9H_2O$ were dissolved in 150 mL of deionized water and poured into a 300-mL 0.5 mg mL^{-1} GO solution. After stirring for 30 min, 60 mL of a 1 mol L^{-1} hydrochloric acid solution was added and stirred magnetically for 5 h. The resulting RGO/S composite was filtered, washed and dried at 60 °C.

0.2 g of the obtained RGO/S composite was dispersed in 50 mL of water with 1 wt% CTAB. Then, 0.05 g of pyrrole was injected into the solution with vigorous stirring for 0.5 h under an ice bath. Next, 7.5 mL of 0.1 mol L^{-1} $FeCl_3$ was added and further stirred for 12 h. The resulting RGO/S@PPy composite was washed and vacuum-dried at 60 °C.

2.2 Material characterization

The surface morphologies of the materials were analysed by FE-SEM, (JSM-6360LV, JEOL). The inner morphologies and elemental distributions of the materials were determined by TEM (Tecnai G2F20 S-TWIX) coupled with energy-dispersive X-ray spectroscopy (EDS). Thermogravimetric analysis (TGA, Netzsch, STA409PC/4/H) was carried out under a N_2flow at10 °C min^{-1}.

2.3 Electrochemical measurements

CR2032-type coin cells were used to evaluate the electrochemical properties of the materials. The working electrodes were prepared via the slurry-coating method, containing 70 wt% synthesized material, 20 wt% acetylene black and 10 wt% polyvinylidenefluoride (PVDF) in NMP. Celgard 2400 film and lithium metal were used as the separator and counter electrode, respectively. A solution of 1 M lithium bis(trifluoromethanesulfonyl)imide (LiTFSI) in DME/DOL (1:1, vl/vl) with 2 wt% $LiNO_3$ was used as the electrolyte. A multi-channel LAND CT2001A battery tester was used to evaluate the electrochemical properties of the materials. The specific capacities of the materials were calculated on the basis of the sulfur content in the cathode. Cyclic voltammetry (CV) was carried out from 1.5-3.0 V at 0.1 mV s^{-1} to characterize the redox behaviour of the composites.

3. RESULTS AND DISCUSSION

Fig. 1a shows the SEM image of stacked RGO/S particles. As displayed in the figure, the surface morphology shows pretty homogenous mixing of sulfur with RGO [28,30,31]. The TEM image of the RGO/S composite is displayed in Fig. 1b, and flexible and corrugated thin layers of graphene sheets can be observed, with no apparent large aggregated particles of sulfur. Fig. 1c presents the SEM image of the RGO/S@PPy composite, which exhibits agglomerated particles and a denser surface structure. The TEM image apparently indicates that the RGO/S composite is coated by a PPy layer (Fig. 1d), which can tightly cover the S nanoparticles on the RGO surface. Moreover, the PPy coating can dramatically increase the mechanical stability of the electrode because its elastic long-chain structure can ease the massive volume changes during cycling.

(a) (b)

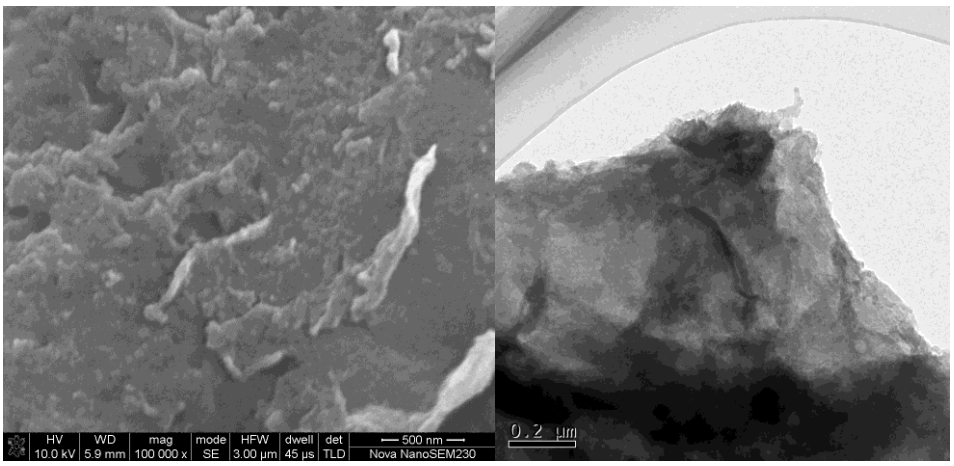

(c) (d)

Figure 1. SEM and TEM images of the prepared RGO/S (a, b) and RGO/S@PPy (c, d) composites

The HRTEM image of RGO/S in Fig. 2a shows that when sulfur is loaded on RGO, the multilayer structure of the graphene sheets still exists in the RGO/S composite. As displayed in the elemental mapping image of RGO/S (Fig. 2b), the signal from the element S is uniformly distributed, confirming the uniform distribution of S on the RGO sheets[32]. The signal of O in both materials may come from the residual oxygen-containing groups in RGO, and the signal of N in RGO/S@PPy comes from the nitrogen functional groups in the PPy coating (Fig. 2c). The uniform distribution of N further indicates the homogeneous coating of PPy on the RGO/S composite. The presence of O- and N-containing functional groups is beneficial for the adsorption of intermediate polysulfides[21,33].

The TG curves of GO, RGO/S and RGO/S@PPy are displayed in Fig. 3. Two major weight loss steps for GO can be observed in Fig.3a. The weight loss occurring before 100 °C could be ascribed to the removal of adsorbed water, while that occurring between 100 and 300 °C is due to the decomposition of labile oxygen functional groups, which is quite consistent with previously reported results [28].

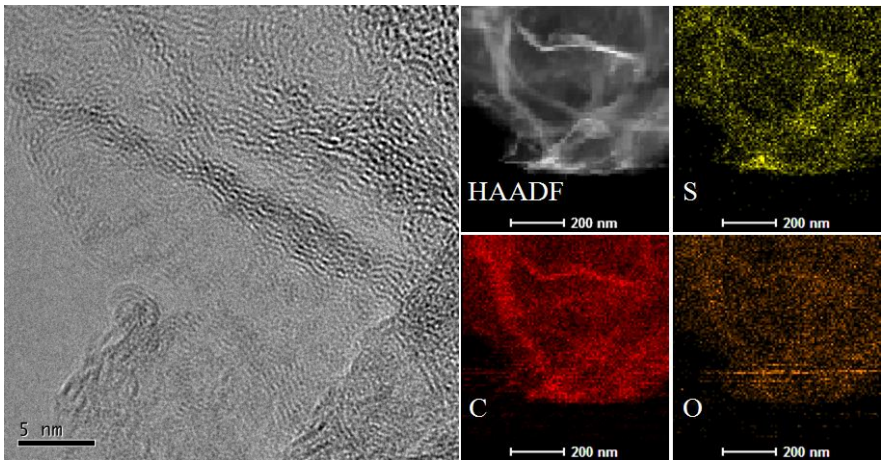

(a) (b)

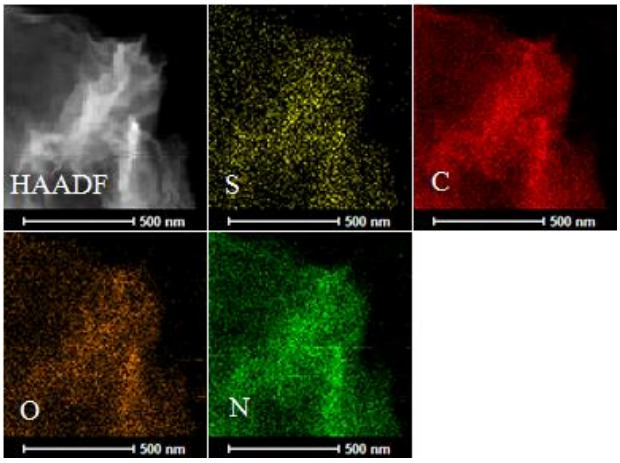

(c)

Figure 2. HRTEM image of RGO/S(a) and elemental mapping of RGO/S (b) and RGO/S@PPy (c) composites

After the reaction, the graphene sheet edges become hydrophobic and a small amount of interlamellar water is trapped, which results in small mass losses for RGO/S and RGO/S@PPy composites below 100 °C (Fig. 3b) [28]. According to previous reports, the weight loss of PPy in the composite could be ignored within the evaporation temperature range of sulfur [27]. Therefore, the weight losses of RGO/S and RGO/S@PPy between 150 °C and 330 °C could be attributed to the evaporation of sulfur[31,34]. The sulfur content was calculated to be 53.4 % in RGO/S and 41.3 % in RGO/S@PPy.

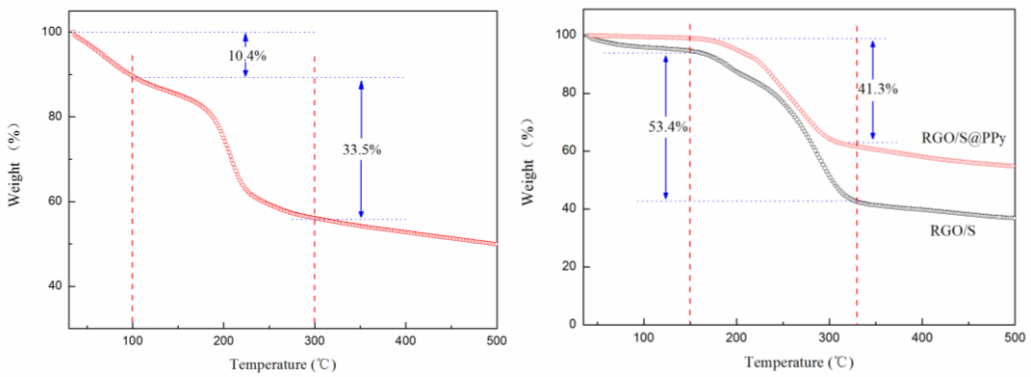

(a) (b)

Figure 3. TG curves of GO (a), RGO/S and RGO/S@PPy (b)

CV curves of the RGO/S@PPy cathode in the first three cycles are presented in Fig. 4. Following the multiple reaction mechanisms of sulfur, the peaks located at 2.34 V and 2.04 V during the cathode scan corresponds to the reduction of cyclic sulfur to high-order lithium polysulfides (Li_2S_x, $4 \leq x \leq 8$) and further to low-order Li_2S_2 and Li_2S. In addition, the anodic peak at 2.50 V corresponds to the reverse reaction of Li_2S/Li_2S_2 and short-chain polysulfides to Li_2S_8 [35,36,37]. The lithiation and

delithiation processes become stable after the first cycle.

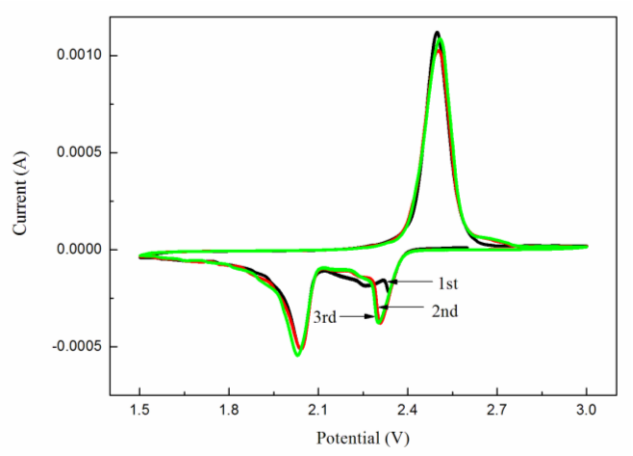

Figure4. CV curves of the RGO/S@PPy electrode in the first three cycles at the scan rate of 0.1 mV s^{-1}

Fig. 5a presents the cycle properties of the composites at 0.2 C. Initial specific capacities of 1031.4 mAh g^{-1} and 1046.3 mAh g^{-1} are obtained for the RGO/S and RGO/S@PPy composites, respectively. The capacity of the RGO/S composite decays rapidly to 435 mAh g^{-1} after 200 cycles, while that of RGO/S@PPy retains 631 mAh g^{-1} even after 300 cycles, with a decrease rate of 0.132% per cycle. Normally, the gradual dissolution of polysulfide anions (S_x^{2-}) leads to a low Coulombic efficiency [38,39]. However, the RGO and PPy in the respective RGO/S and RGO/S@PPy samples can prevent the loss of polysulfide species in the electrolyte. Thus, both the RGO/S and RGO/S@PPy samples show an excellent Coulombic efficiency of nearly 100%. The improved cycling stability of RGO/S@PPy could be ascribed to the uniform PPy coating, which can further relieve the dissolution of polysulfides into the electrolyte.

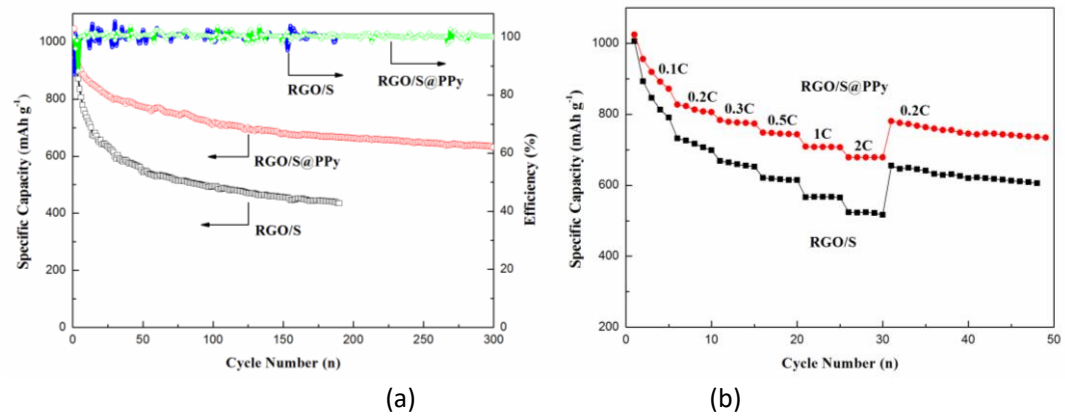

Figure 5. Cycling properties of the RGO/S and RGO/S@PPy electrodes at 0.2 C and their Coulombic efficiencies (a); rate performance of the RGO/S and RGO/S@PPy electrodes (b)

The rate performance of the composites is shown in Fig. 5b. The corresponding average

discharge capacities at 0.1 C, 0.2 C, 0.3 C, 0.5 C, 1 C and 2 C for RGO/S and RGO/S@PPy are 847.0, 717.1, 659.1, 616.5, 567.1, 523.9 mAh $g^{-1}$and 918.9, 813.6, 776.4, 745.9, 707.7, and 678.6 mAh g^{-1}, respectively. As the discharge current is switched to 0.2 C again, capacities of 655.0 and 780.6 mAh g^{-1} are achieved for RGO/S and RGO/S@PPy, respectively. The RGO/S@PPy material shows considerably higher specific capacities than the RGO/S composite at different discharge rates, indicating the improved utilization of sulfur caused by the PPy coating.

4. CONCLUSION

An RGO/S@PPy composite has been prepared via a facile synthesis method. The results demonstrate that sulfur is uniformly distributed on the RGO sheets, and a PPy layer is homogeneously coated on the surface of the RGO/S composite. The PPy coating relieves the dissolution of polysulfides and improves the utilization of active sulfur. As a result, a discharge capacity of 631 mA h g^{-1} after 300 cycles at 0.2 C and an excellent rate capability are obtained. This finding indicates that the prepared RGO/S@PPy composite is promising for application in Li-S batteries.

ACKNOWLEDGMENTS
This work was supported by the Natural Science Foundation of Hunan Province, China (2018JJ3176).

References

1. J. D. Zhu, P. Zhu, C. Y. Yan, X. Dong and X. W. Zhang, *Prog. Polym. Sci.,* 90(2019)118.
2. H. S .Song, A. P. Tang, G. R. Xu, L. H. Liu, M. J. Yin and Y. J. Pan, *Int. J. Electrochem. Sci.,* 13(2018)4720.
3. C. F. Shi, K. X. Xiang, Y. R. Zhu, X. H. Chen, W. Zhou and H. Chen, *Electrochim. Acta,* 246(2017)1088.
4. M. J. Yin, H. S. Song, A. P. Tang, G. R. Xu, L. H. Liu and Y. J. Pan, *Ionics,* 25 (2019)2087.
5. H. S. Song, A. P. Tang, G. R. Xu, L. H. Liu, Y. J. Pan and M. J. Yin, *Int. J. Electrochem. Sci.,* 13(2018)6708.
6. F. Wu, S. Y. Zhao, L. Chen, Y. Lu, Y. F. Su, J. Li, L. Y. Bao, J. Y. Yao, Y. W. Zhou and R. J. Chen, *Electrochim. Acta,* 292(2018)199.
7. M. D. Walle, K. Zeng, M. Y. Zhang, Y. J. Li and Y. N. Liu, *Appl. Surf. Sci.*,473(2019)540.
8. S. Y. Lang, R. J. Xiao, L. Gu, Y. G. Guo, R. Wen and L. J. Wan, *J. Am. Chem. Soc.*,140(2018)8147.
9. J. Wu, S. Y. Li, P. Yang, H. P. Zhang, C. Du, J. M. Xu and K. X. Song, *J. Alloy. Compd.,* 783(2019)279.
10. Z. P. Ma, F. Y. Jing, Y. Q. Fan, J. J. Li, Y. Zhao and G. J. Shao, *J. Alloy. Compd.,* 789(2019)71.
11. J. J. Yuan, X. K. Zheng, L. Jiang, D. C. Yao, G. Y. He, H. Q. Chen and J. F. Che, *Mater. Lett.,* 219(2018)68.
12. J. H. Song, J. M. Zheng, S. Feng, C. X. Zhu, S. F. Fu, W. G. Zhao, D. Du and Y. H. Lin, *Carbon,* 128(2018)63.
13. H. Lu, Z. Chen, Y. Yuan, H. L. Du, J. L. Wang, X. Liu, Z. Z. Hou, K. Zhang, J. Fang and Y. H. Qu, *J. Electrochem. Soc.,* 166(2019)A2453.
14. H. S. Song, Y. J. Pan, A. P. Tang, G. R. Xu, L. H. Liu and H. Z. Chen, *Ionics,* 25(2019)3121.
15. Y. Z. Zhang, X. L. Zong, L. Zhan, X. Y. Yu, J. Gao, C. C. Xun, P. Y. Li and Y. L. Wang, *Electrochim. Acta,* 284(2018)89.

16. C. X. Li, J. Y. Yu, S. L. Xue, Z. H. Cheng, G. Q. Sun, J. Zhang, R. D. Huang and L. T. Qu, *Carbon,* 139(2018)522.
17. Y. Q. Wang, S. Q. Luo, D. Q. Wang, X. B. Hong and S. K. Liu, *Electrochim. Acta,* 284(2018)400.
18. Z. H. Cao, C. Q. Wang and J. Chen, *Mater. Lett.,* 225(2018)157.
19. W. B. Kong, D. T. Wang, L. J. Yan, Y. F. Luo, K. L. Jiang, Q. Q. Li, L. Zhang, S. G. Lu, S. S. Fan, J. Li and J. P. Wang, *Carbon,* 139(2018)896.
20. H. W. Wu, Y. Huang, M. Zong, H. T. Fu and X. Sun, *Electrochim. Acta,* 163(2015)24.
21. W. W. Qian, Q. M. Gao, H. Zhang, W. Q. Tian, Z. Y. Li and Y. L. Tan, *Electrochim. Acta,* 235(2017)32.
22. L. Ma, K. E. Hendrickson, S. Y. Wei and L. A. Archer, *Nano Today,* 10(2015)315.
23. X. W. Wang, Z. A. Zhang, X. L. Yan, Y. H. Qu, Y. Q. Lai and J. Li, *Electrochim. Acta,* 155(2015)54.
24. S. Huang, R. T. Guan, S. J. Wang, M. Xiao, D. M. Han, L. Y. Sun and Y. Z. Meng, *Prog. Polym. Sci.,* 89(2019)19.
25. Y. G. Zhang, Y. Zhao, A. Konarov, D. Gosselink, H. G. Soboleski and P. Chen, *J. Power Sources,* 241(2013)517.
26. C. H. Wang, H. W. Chen, W. L. Dong, J. Ge, W. Lu, X. D. Wu, L. Guo and L. W. Chen, *Chem. Commun.,* 50(2014)1202.
27. W. Yang, W. Yang, J. N. Feng, X. J. Qin and Q. W. Tang, *J. Energy Chem.,* 27(2018)813.
28. H. Sun, G. L. Xu, Y. F. Xu, S. G. Sun, X. F. Zhang, Y. C. Qiu and S. H. Yang, *Nano Res.*,5(2012)726.
29. D. C.Marcano, D. V.Kosynkin, J. M. Berlin, A.Sinitskii, Z. Z. Sun, A.Slesarev, L. B.Alemany, W. Lu and J. M. Tour, *ACS Nano,* 4(2010)4806.
30. S. Moon, Y. H. Jung and D. K. Kim, *J. Power Sources,* 294(2015)386.
31. W. Wang, G. C. Li, Q. Wang, G. R. Li, S. H. Ye and X. P. Gao, *J. Electrochem. Soc.,* 160(2013)A805.
32. C. Wang, J. J. Chen, Y. N. Shi, M. S. Zheng and Q. F. Dong, *Electrochim. Acta,* 55(2010)7010.
33. L. W. Ji, M. M. Rao, H. M. Zheng, L. Zhang, Y. C. Li, W. H.Duan, J. H. Guo, E. J. Cairns and Y. G. Zhang, *J. Am. Chem. Soc.,* 133 (2011)18522.
34. Y. G. Zhang, L. C. Sun, H. P. Li, T. Z. Tan and J. D. Li, *J. Alloy. Compd.,* 739(2018)290.
35. H. S. Song, Q. J. Kuang, H. L. Yuan, H. Z. Chen, G. R. Xu, A. P. Tang and L. H. Liu, *Mater. Express,* (2020), DOI: https://doi.org/10.1166/mex.2020.1808.
36. N. Li, F. Y. Gan, P. Wang, K. H. Chen, S. Y. Chen and X. He, *J. Alloy. Compd.,* 754(2018)64.
37. Z. J. Guo, X. Y. Feng, X. X. Li, X. M. Zhang, X. Peng, H. Song, J. J. Fu, K. Ding, X. Huang and B. Gao, *Front. Chem.,* 6(2018)429.
38. H. S. Song, H. L. Yuan, H. Z. Chen, A. P. Tang, G. R. Xu, L. H. Liu, Z. A. Zhang and Q. J.Kuang, *J. Solid State Electr.,* 24(2020)997.
39. P. Wei, M. Q. Fan, H. C. Chen, X. R. Yang, H. M. Wu, J. D. Chen, T. Li, L. W. Zeng and Y. J. Zou, *Electrochim. Acta*,174(2015)963.